Journal of Thermal Analysis, Vol. 48 (1997) 1325-1336

THERMAL INVESTIGATION OF COBALT, NICKEL AND COPPER COMPLEXES WITH 8-AMINOQUINOLINE
Correlation between thermal stability and crystal field splitting energy

A. M. Donia[*] *and H. A. El-Boraey*

Department of Chemistry, Faculty of Science, Menoufia University, Shebin El-Kom, Egypt

(Received December 6, 1995; in revised form August 11, 1996)

Abstract

Complexes of Co(II), Ni(II) and Cu(II) with 8-aminoquinoline were prepared and characterized, and their thermal behaviour and decomposition pathways were studied. The thermal stabilities are discussed in terms of ionic radii, crystal field splitting energy and steric hindrance. The effective roles of the counter-ions (Cl^- and NO_3^-) on the decomposition temperatures and the final products were also clarified. The energies of activation (E_a) and the orders of some decomposition reactions were determined. Light is shed on the nature of the interaction of the water of crystallization and the polymorphic transformation phenomenon.

Keywords: 8-aminoquinoline complexes, thermal investigation

Introduction

Thermal decomposition studies on metal complexes have demonstrated various correlations of the decomposition temperature with the metal ion, the ligand character or the counter-ion [1–6]. A literature survey reveals that little work has been done on the metal complexes of 8-aminoquinoline and their thermal properties [7–10]. We recently reported the effect of precipitation on the thermochromic behaviour of nickel(II) complexes with 8-aminoquinoline [11]. Our present work has been devoted to the characterization and thermal investigation of other metal 8-aminoquinoline complexes. The work also concerns the effects of the ionic radii and crystal field splitting energies (10 Dq) on the thermal stabilities of the isostructural octahedral nitrato complexes.

---

[*] Author to whom all correspondence should be addressed.

0368–4466/97/ $ 5.00

John Wiley & Sons Limited
Chichester

Experimental

All reagents were of analytical grade; they were obtained from Aldrich and used without further purification. Complexes 1–5 were prepared by addition of the stoichiometric amount of the hydrated metal chloride or nitrate salt in EtOH to a solution of the ligand in $CHCl_3$ at a 1:2 molar ratio, and the reaction mixtures were stirred in air at room temperature for 2 h. The precipitates obtained were filtered off, washed several times with $CHCl_3$ and dried over $CaCl_2/P_4O_{10}$. The copper complex 6 was prepared by the same method, except that the molar ratio was 1:1. The elemental analyses (C and H) were performed at the Micro-Analytical Centre of Cairo University. The metal contents in the respective metal complexes were determined complexometrically, gravimetrically (DMG) and iodometrically for cobalt, nickel and copper, respectively. IR spectra were recorded by using KBr discs and a Perkin-Elmer 1430 spectrophotometer. Electronic spectra were registered with a Perkin-Elmer Lambda 4B spectrophotometer. Magnetic susceptibility measurements were carried out at room temperature on a modified Gouy type magnetic balance. Conductivity measurements on the complexes were performed in EtOH or MeOH at a concentration of 10^{-3} *M* with a Tacussel CD6N conductimeter. The thermal analyses (DTA and TG) were carried out in air with a Simadzu DT-40 thermal analyser, at a heating rate of 10°C min^{-1}. X-ray diffraction measurements were made with a Simadzu XD-3 diffractometer with CuK_α radiation.

Results and discussion

The complexes are stable in air and soluble in water and some organic solvents. The nitrato complexes do not melt, but decompose above 180°C. The chloro complex 6 melts at 240°C. The chloro complexes 4 and 5 change into green tetrahedral complexes upon heating in mull and dissolution in DMF or CH_3CN, showing thermochromic and solvatochromic behaviour. This transformation is attributed to the loss of one ligand molecule, as demonstrated by thermal and spectral measurements. The molar conductances (Table 1) indicate the non-electrolytic nature of the complexes [12].

Vibrational spectra

The bands observed for the ligand and its complexes are listed in Table 1. The ligand exhibits bands at 1610, 1595, 1560 and 1465 cm^{-1}, assigned to $\nu(\mathrm{C}\overset{\cdots}{-}\mathrm{C})+$ $+\nu(\mathrm{C}\overset{\cdots}{-}\mathrm{N})$ of the quinoline ring; these are shifted to higher frequencies for the complexes. The ring vibrations at 980 and 380 cm^{-1} for the free ligand also shift to higher frequencies (990 and 430 cm^{-1}). These observations suggest coordination through the quinoline ring nitrogen [13–15]. The complexes also display bands at ca. 3320–3040 and 1315 cm^{-1}, assigned to coordinated $\nu(NH_2)$ and ν(C–N), respectively. We therefore conclude that the ligand is bidentate, chelating through both nitrogen atoms. The nitrato complexes give additional bands at ca. 1380, 1350 and 1025 cm^{-1}, which are assigned to monodentate nitrate [16].

Electronic spectra

The electronic spectra of the complexes are recorded in Table 1. The bands observed for the Co(II) and Ni(II) complexes within the range 800–410 nm confirm octahedral geometry around the metal ions [17–19]. This is supported by the magnetic moment values at room temperature (Table 1), which are typical for octahedral geometry [15, 17, 20]. The Cu(II) complexes 3 and 5 display bands near 585 and 410 nm, which are assigned to octahedral geometry [17–19], while complex 6 exhibits a broad band with a maximum at 700 nm, indicating tetrahedral geometry [17]. The above findings, together with the results of the elemental analyses and the TG data, indicated that the following structures became more significant.

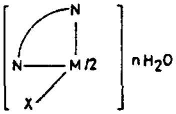

1: M=Co, X=NO$_3$, n=2; 2: M=Ni, X=NO$_3$, n=2;
3: M=Cu, X=NO$_3$, n=0; 4: M=Co, X=Cl, n=2;
5: M=Cu, X=Cl, n=2

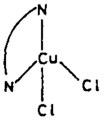

$\left(^{N}_{N}\right>$8-aminoquinoline (L) (6)

Thermal studies

The DTA curve of the ligand (Fig. 1) shows endothermic peaks at ca. 72°C (sharp) and 160–265°C (split). These peaks are assigned to melting and volatilization with decomposition, respectively (as shown on a hot-stage microscope).

Nitrato-complexes (1–3)

The DTA curves of the cobalt and nickel complexes 1 and 2 display an endothermic peak in the temperature range 69–122°C, corresponding to the loss of water of crystallization. The mass losses obtained from TG (Table 2) confirm the loss of two molecules of water. The lower temperature of desolvation, together with the slight differences in the IR spectra of the complexes before and after desolvation, indicate the weak interaction of the water of crystallization, i.e. the water makes no contribution to the lattice forces and is trapped in the crystal voids [21, 22]. The exothermic peak (120–150°C) observed in the DTA curve of the copper complex 3 may be attributed to a phase change, as deduced from TG, which shows no mass loss in this temperature range (Fig. 1). The X-ray patterns of the complex and its heated form

Table 1 Analytical, magnetic and spectral data of the complexes

Compound	Colour	Found (calcd.)/%			μ_{eff}/ B.M.	Λ_m /cm$^2\Omega^{-1}$mol^{-1} in EtOH
		C	H	M		
8-aminoquinoline (L)						
[$CoL_2(NO_3)_2$]·$2H_2O$	brown	42.1	4.2	11.1	4.32	43.8
		(42.6)	(3.9)	(11.6)		
[$NiL_2(NO_3)_2$]·$2H_2O$	pale	42.9	3.9	11.0	3.00	44.8
	violet	(42.6)	(3.9)	(11.6)		
[$CuL_2(NO_3)_2$]	blue	44.6	3.4	13.7	1.65	insoluble
		(45.4)	(3.4)	(13.3)		
[CoL_2Cl_2]·$2H_2O$	light	47.5	4.4	13.4	4.93	110^c
	brown	(47.5)	(4.4)	(12.9)		
[CuL_2Cl_2]·$2H_2O$	blue	47.7	4.4	13.6	1.57	–
		(47.0)	(4.4)	(13.8)		
[$CuLCl_2$]	green	39.0	3.0	22.6	1.72	–
		(38.7)	(2.9)	(22.7)		

Table 1 Continued

Compound	IR/cm^{-1}					Electronic spectra in mull/nm	
	$\nu_{(NH_2)}$	$\nu_{(C\overset{\cdots}{-}C)}+\nu_{(C\overset{\cdots}{-}C)}$	$\nu_{(C-N)}$	ring vibration	$\nu_{(NO_3^-)}$	*d–d*	other bands
8-aminoquinoline (L)	3440–3340^a	1610–1595^a	1330 s	980 w			
		1560 s		380 br			
		1465 m					
[CoL$_2$(NO$_3$)$_2$]·2H$_2$O	3290–3100^a	1640–1625^a	1315 m	985 sh	1380 s	^{b} 800–600 sh	^{b} 400–350 sh, 310 m
		1590–1570^a		420 m	1350 m	476 s	^{b} 250 s, 240–200^a
		1470 m			1025 m		
[NiL$_2$(NO$_3$)$_2$]·2H$_2$O	3320–3100^a	1640–1630^a	1315 m	985 m	1380 s	560 m	300 m 280 m 225 s
		1590–1570^a		420 m	1350 sh	440–410^a	
		1470 m					
[CuL$_2$(NO$_3$)$_2$]	3440–3070^a	1630 m	1315 m	985 m	1380 s	585 s	370 w, 280 m, 260 m
		1590–1570^a		420 m	1330 m	410 s	250 s
		1470 m					
[CoL$_2$Cl$_2$]·2H$_2$O	3295–3090^a	1640–1620^a	1315 s	995 m	–	^{c} (600–440 sh)	^{c} (340 m, 250 s)
		1590–1570^a		420 m	–		
		1465 m					
[CuL$_2$Cl$_2$]·2H$_2$O	3470–3040^a	1645–1620^a	1315 s	990 m	–	580 s	380 m, 340 s, 330 m
		1590–1580^a		420 m			
		1475 s					
[CuL$_2$Cl$_2$]	3220–3100^a	1640–1615^a	1310 s	990 w	–	700 s	390 s, 370 m,
		1585 s		420 w			300–240 br
		1555 m					
		1465 m					

^{a} split; ^{b} in Et OH; ^{c} in Me OH.

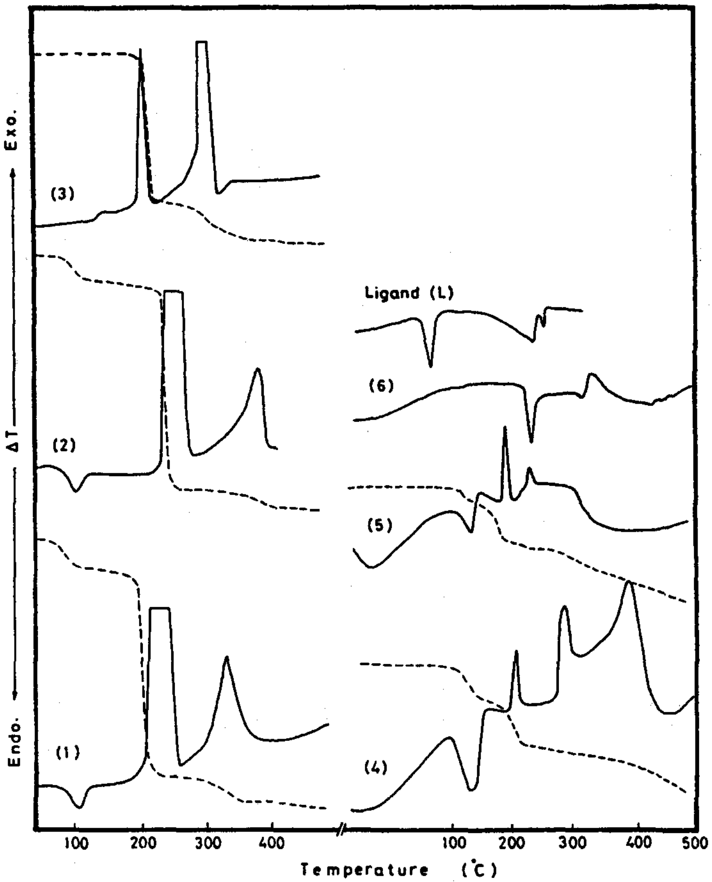

Fig. 1 DTA and TG curves of the ligand and the complexes

are different (Fig. 2), confirming the phase change. Moreover, the IR spectra of the complex and its heated form exhibit significant differences, especially for $\nu(NH_2)$, $\nu(\mathrm{C}\overset{\cdots}{=}\mathrm{C})+\nu(\mathrm{C}\overset{\cdots}{=}\mathrm{N})$, $\nu(NO_3)$ and the ring vibrations. These changes may be attributed to a polymorphic transformation [21, 22]. The curves of the complexes also display a number of exothermic peaks in the temperature range 173–380°C, which are assigned to material decomposition. The mass losses (Table 2) indicate that the decomposition starts with the scission of M–N bonds, giving the free ligand and anhydrous metal nitrates, which are spontaneously decomposed in the same temperature range. The formation of metal nitrate during the decomposition pathways was confirmed by the IR spectra of the complexes after heating up to 215°C (initial period of the reaction). The spectra show a sharp, strong $\nu(NO_3)$ at 1380 cm^{-1}, whereas the characteristic peaks of the ligand have disappeared. Moreover, the sequence of the decomposition reactions and their corresponding defined steps as deduced from the TG and DTA curves (Fig. 1 and Table 2) are presented below.

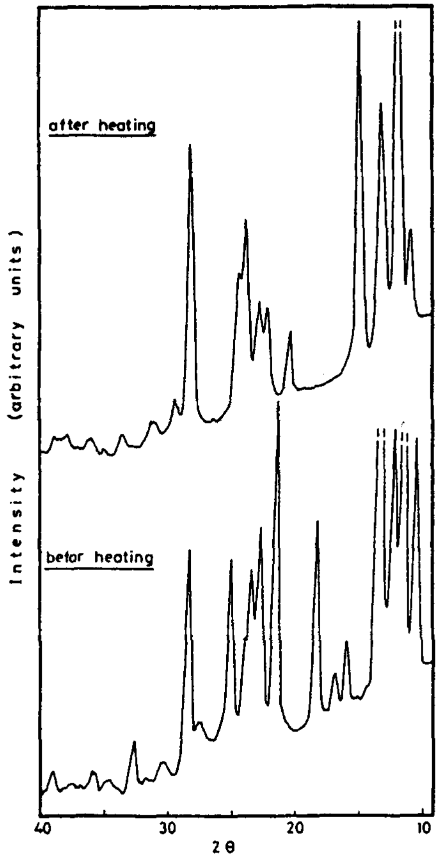

Fig. 2 X-ray patterns of Cu(II) complex (3) before and after heating

a) Co-complex

$$[CoL_2(NO_3)_2]\cdot 2H_2O \xrightarrow{69-122^\circ C} CoL_2(NO_3)_2 + 2H_2O \qquad (1)$$

$$3CoL_2(NO_3)_2 \xrightarrow{173-237^\circ C} 6L + 3NO_2 + 0.5O_2 + $$
$$+ 0.5Co_3O_4 + 3/2Co(NO_3)_2 \qquad (2)$$

$$3Co(NO_3)_2 \xrightarrow{290-374^\circ C} 6NO_2 + O_2 + Co_3O_4 \qquad (3)$$

b) Ni-complex

$$[NiL_2(NO_3)]_2\cdot 2H_2O \xrightarrow{72-120^\circ C} NiL_2(NO_3)_2 + 2H_2O \qquad (1)$$

$$3NiL_2(NO_3)_2 \xrightarrow{242-274^\circ C} 6L + 6NO_2 + 3/2O_2 + 3NiO \qquad (2)$$

c) Cu-complex

$$2CuL_2(NO_3)_2 \xrightarrow{199-289^\circ C} 4L + 2NO_2 + 0.5O_2 + CuO + Cu(NO_3)_2 \qquad (1)$$

$$Cu(NO_3)_2 \xrightarrow{305-374^\circ C} 2NO_2 + 0.5O_2 + CuO \qquad (2)$$

It is seen from the above results that the cobalt and copper complexes lose their ligand molecules in the first decomposition step. The metal nitrates obtained decompose in one or two steps according to their rate and temperature of decomposition. The decomposition reactions of all complexes are of first order (Table 3), as indicated by the peak asymmetry method of Kissinger [23]. The energies of activation (E_a) of these reactions are also listed in Table 3, as found by the method of Piloyan *et al.* [24] (Fig. 3). The temperatures of initial decomposition (thermal stability) of the complexes follow the sequence Ni>Cu>Co (Table 2).

Table 2 DTA and TG data of the complexes

Complex	Temperature range/°C		Mass loss/%	Reaction
	DTA	TG	Found (calcd.)	
(1)	69–122*	69–122	7.2 (7.1)	a
	187–237 (exo)	173–237	66.5 (67.0)	b
	290–374 (exo)	290–374	8.5 (10.1)	c
(2)	72–120*	72–120	7.3 (7.1)	a
	242–274 (exo)	242–274	79.1 (78.3)	b
(3)	120–150*			phase change
	199–289 (exo)	199–289	73.0 (72.0)	b
	305–374 (exo)	305–374	11.7 (11.4)	c
(4)	90–150	90–205	39.0 (39.6)	formation of
	195–220 (exo)			tetrahedral ($CoLCl_2$)
	220–500 (exo)	205–480	41.0 (42.6)	b
(5)	90–150*	80–240	40.0 (39.2)	formation of
	190–245 (exo)			tetrahedral ($CuLCl_2$)
	300–500	270–480	32.0 (31.4)	b
(6)	240*			melting
	310–390 (exo)			b

a desolvation
b decomposition
c completion of decomposition of metal nitrate obtained
* endo

Table 3 Initial temperature of decomposition, ionic radii (r^{2+}), crystal field splitting energy (10 Dq), activation energy (E_a) and order of reactions ($\bar{n}$)

Complex	Initial temp. of decomp./°C	r^{2+}/Pm	10 Dq/ kJ mol^{-1}	E_a/ kJ mol^{-1}	$\bar{n}$
1	173	74	199	170.4	1.06
2	242	69	213	207.9	1.10
3	199	72	204	232.8	1.09

(10 Dq calculated from the electronic spectra of complexes)

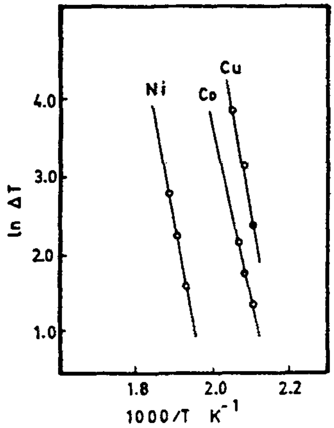

Fig. 3 Plots constructed from the DTA curves of nitrato-complexes

The effective role of the central metal ion in the thermal stabilities was confirmed by the correlation between both ionic radii and the crystal field splitting energy (10 Dq), and the temperature of initial decomposition (Fig. 4). It is seen that as the ionic radii decrease (higher charge/radius ratio), the thermal stability increases. This can be explained by the higher metal-ligand interaction, which results in a higher crystal field splitting energy (Table 3). Since the complexes are isostructural, the correlation obtained between 10 Dq and the decomposition temperature confirms that the ionic radius is the only factor affecting the metal-ligand interaction (bond strength).

Chloro-complexes

The chloro complexes (except 6) have lower thermal stabilities than the nitrato complexes. The octahedral complexes 4 and 5 change into green tetrahedral 4a and 5a in both the solid state (upon heating in mulls up to 120°C) and solution. The thermal studies indicate that the geometry change can be attributed to the loss of one ligand molecule and water of crystallization. The electronic spectra of 4a and 5a show bands at 670–610 and 700 nm, respectively. These bands are assigned to

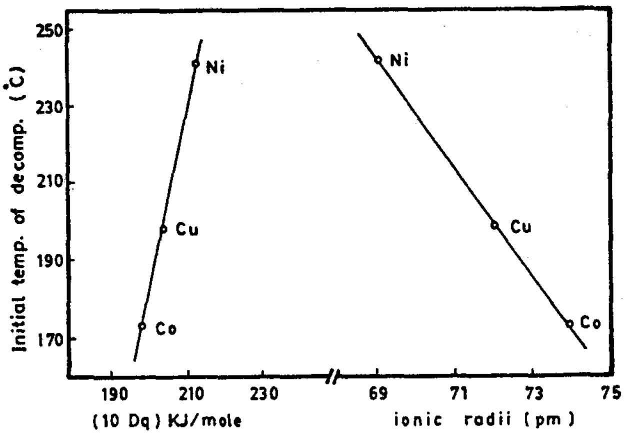

Fig. 4 A plot of ionic radii and crystal field splitting energy with the initial temperature of decomposition of nitrato-complexes

tetrahedral geometry [17]. On the other hand, the IR spectra of the complexes are typically consistent with that of the green tetrahedral complex 6. The DTA curves of complexes 4 and 5 (Fig. 1) reveal an endothermic peak at 90–150°C, which is assigned to the loss of water of crystallization together with the melting and partial volatilization of the separated ligand molecule. The exothermic peak observed in the interval 195–245°C is assigned to the completion of decomposition of the ligand molecule to give the tetrahedral complexes with formula $MLCl_2$, which in turn start to decompose at 205 and 270°C for 4 and 5, respectively. The higher thermal stability of the copper complex than that of cobalt is in accordance with the above observation for the nitrato complexes. On the other hand, the following pathways of the decomposition reactions are suggested, as demonstrated by the TG and DTA data (Table 2):

a) Co-complex

$$[CoL_2Cl_2]\cdot 2H_2O \xrightarrow{90-205^{\circ}C} CoLCl_2 + L + 2H_2O \qquad (1)$$

$$CoLCl_2 + 2/3O_2 \xrightarrow{205-480^{\circ}C} L + Cl_2 + 1/3Co_3O_4 \qquad (2)$$

b) Cu-complex

$$[CuL_2Cl_2]\cdot 2H_2O \xrightarrow{80-240^{\circ}C} CuLCl_2 + L + 2H_2O \qquad (1)$$

$$CuLCl_2 \xrightarrow{270-480^{\circ}C} CuCl_2 + L \qquad (2)$$

Finally, and from the above arguments, the following points are considered.

i) The nitrato complexes give the metal oxides at lower temperatures than those for the chloro complexes. This may be attributed to the oxidation effect of the nitrate anion.

ii) The octahedral nitrato-complexes have higher thermal stabilities than the corresponding chloro complexes. This may be attributed to the distribution of the ligands around the metal as shown in Scheme 1 (molecular models indicate that the ligand coordinates in two perpendicular planes).

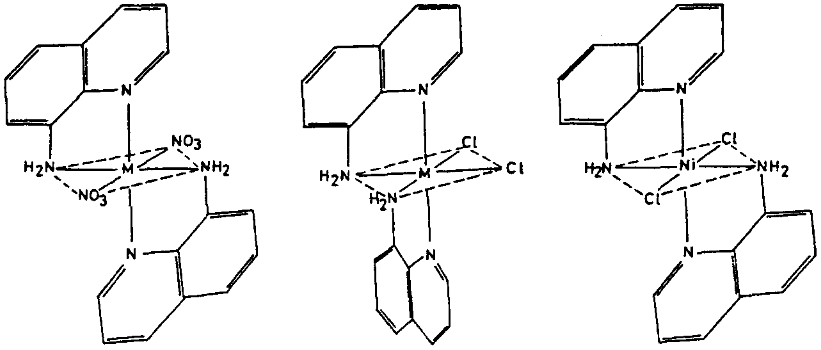

Scheme 1

According to the above scheme, the chloro complexes exhibit a higher steric hindrance, which leads to the loss of one ligand molecule to relieve the strain in the molecule. This explanation can be confirmed by the higher thermal stability (above 300°C) of the octahedral chloro-complex of the nickel analogues [11].

References

1 G. Liptay, E. Papp-Molnár and K. Burger, J. Inorg. Nucl. Chem., 31 (1969) 247.
2 R. A. Bailey and W. J. Tangredi, J. Inorg. Nucl. Chem., 38 (1976) 2221.
3 R. Lozano, J. Martinez, A. Martinez and A. Doadrio Lopez, Polyhedron, 2 (1983) 977.
4 A. M. Donia, M. I. Ayad and R. M. Issa, Transition Met. Chem., 16 (1991) 518.
5 A. M. Donia, M. Goda, M. I. Ayad and H. El-Boraey, Thermochim. Acta, 194 (1992) 155.
6 A. M. Donia, S. A. Amer, R. M. Issa and M. Gaber, Transition Met. Chem., 15 (1990) 465.
7 Y. Kidani, Y. Oya and K. Inagaki, Yakugaku Zasshi, 97 (1977) 932.
8 M. M. Abou Sekkina and S. M. El-Helbawy, Thermochim. Acta, 81 (1984) 223.
9 J. Casabo, M. Izquierdo, J. Ribas and C. Diaz, Transition Met. Chem., 8 (1983) 110.
10 C. Engelter, E. G. Tackson, L. C. Knight and A. D. Thornton, J. Coord. Chem., 20 (1989) 297.
11 A. M. Donia and H. El-Boraey, Transition Met. Chem., 17 (1992) 307.
12 T. Radhakrishnan, P. T. Joseph and C. P. Prabhakaran, J. Inorg. Nucl. Chem., 38 (1975) 2217.
13 R. J. H. Clark and C. S. Williams, Spectrochim. Acta, 22 (1966) 1081.
14 M. A. S. Goher and A. K. Haffz, Acta Chim. Hung., 121 (1986) 363.
15 N. Saha and D. Mukherjee, Polyhedron, 2 (1983) 47.
16 K. Nakamoto, Infrared and Raman Spectra of Inorganic and Coordination Compounds, A. Wiley Interscience, 3rd edition, New York 1977.
17 R. J. Duff, J. Chem. Soc., (a) (1968) 434.
18 A. B. P. Lever, Inorganic Electronic Spectroscopy, Elsevier, Amsterdam 1968.

19 R. C. Aggarwall, A. R. Rai and T. R. Rao, J. Inorg. Nucl. Chem., 43 (1981) 1927.
20 J. R. Majer and A. S. P. Azzouz, J. Inorg. Nucl. Chem., 43 (1981) 1793.
21 S. B. Pyran, Solid State Chemistry of Drugs. Academic Press, New York, London 1982.
22 A. M. Donia, S. Abou El-Enein and M. S. Masoud, Thermochim. Acta, 161 (1990) 217.
23 H. E. Kissinger, Anal. Chem., 29 (1957) 1702.
24 G. O. Piloyan, I. D. Ryabchikov and O. S. Novikova, Nature, (1966) 1229.